Available online at www.sciencedirect.com
SCIENCE DIRECT
Molecular Brain Research 116 (2003) 59–69
MOLECULAR BRAIN RESEARCH
www.elsevier.com/locate/molbrainres

Research report

Protein analysis in the rat auditory brainstem by two-dimensional gel electrophoresis and mass spectrometry

Hans Gerd Nothwang*, Michael Becker, Kornelia Ociepka, Eckhard Friauf

Abteilung Tierphysiologie, Universität Kaiserslautern, FB Biologie, Postfach 3049, 67653 Kaiserslautern, Germany

Accepted 15 May 2003

Abstract

A catalogue of the protein repertoire of processing centres in the central auditory system would greatly foster our knowledge on the anatomical and functional properties of this sensory system. Towards this goal, we report on the first mapping study of the protein content in the superior olivary complex (SOC) and the inferior colliculus (IC) of the rat auditory brainstem. The protein content of these two structures was assessed by means of two-dimensional gel electrophoresis (2-DGE) and mass spectrometry. To do so, proteins were first separated into four fractions by differential centrifugation. For comparison, corresponding cerebellar fractions were also analysed. Immunoblot analysis revealed highly enriched microsomal and cytosolic fractions; the other two fractions were mixtures of various subcellular compartments. Separation of the 800 *g* pellets (enriched for nuclear and plasma membrane proteins) and the 100 000 *g* supernatants (enriched for cytosolic proteins) by 2-DGE yielded between 456 and 674 distinct protein spots after silver staining. The overall protein pattern of all three tissues was similar for a given fraction. Fifty prominent protein spots of the SOC cytosolic fraction were identified by mass spectrometry and yielded information on thirty different genes with various cellular functions, e.g. primary metabolism, cytoarchitecture, and signal transduction. Sequencing of eleven corresponding spots from the SOC and IC cytosolic fractions confirmed the great similarity between the two samples. The results of this analysis are part of a novel integrated database of the gene repertoire of the auditory brainstem (ID-GRAB), that is publicly available (http://www.id-grab.de).

Theme: Sensory system

Topic: Auditory systems: central physiology

Keywords: Auditory brainstem; Subcellular fractionation; Mass spectrometry; Two-dimensional gel electrophoresis; Proteomics

1. Introduction

The central auditory system is composed of a high number of centres that perform essential functions in sound localization, pattern recognition, processing of complex sounds, echo suppression and sound perception (for review see [27]). Their analysis, therefore, is a prerequisite for the understanding of normal and impaired hearing conditions with a central auditory component, such as presbyacusis and auditory processing disorders [4,11].

Among the numerous auditory centres, the superior olivary complex (SOC) and the inferior colliculus (IC), which are situated in the mammalian brainstem, represent anatomically and functionally well-defined structures. The SOC is the first central auditory centre receiving input from both ears. It is located in the medullary brainstem and consists of several nuclei, with the major ones being the lateral superior olive (LSO), the medial superior olive (MSO), and the medial nucleus of the trapezoid body (MNTB). Most of the nuclei are involved in binaural sound localization (for reviews see [13,15]). For instance, LSO and MNTB neurons are involved in analysing interaural level differences (ILD), and MSO neurons in interaural time differences (ITD). Both cues are important for sound localization in the horizontal plane. The SOC represents one of the rare cases where the behavioural function of a circuit in the central nervous system is well known (for review see [37]).

The IC is a mesencephalic integration centre that obtains inputs from lower brainstem and forebrain nuclei via

*Corresponding author. Tel.: +49-631-205-4669; fax: +49-631-205-4684.
E-mail address: nothwang@rhrk.uni-kl.de (H.G. Nothwang).

0169-328X/03/$ – see front matter
doi:10.1016/S0169-328X(03)00234-1

anatomically distinct ascending and descending pathways, respectively. IC neurons demonstrate a sophisticated level of coding for complex signals. They respond to amplitude modulation, species-specific vocalizations, and to spatial localization cues (for review see [3]). Recently, the IC was associated with an age-related decline in temporal processing [35].

Despite the importance of central auditory processing centres, the molecular machinery which ultimately determines their function is largely unknown. Differential gene expression forms the basis of tissue specificity. Historically, gene expression has been examined on the level of single genes. The availability of genomic sequences and expressed sequence tags of man and several model organisms, together with the emergence of novel techniques, has recently paved the way for efficient large-scale analysis of gene expression both on the nucleic acid and protein level.

One of the so-called proteomics approaches is based on two-dimensional gel electrophoresis (2-DGE). The great strength of this technique is that it allows to simultaneously separate and visualize hundreds of proteins, including those with different post-translational modifications. At present, no other technique can achieve this. In combination with mass spectrometry, it allows a comprehensive analysis of the protein content (proteome) of a given biological system [24]. Interestingly, the auditory system has a long tradition in proteome analysis; almost 25 years ago, the first 2-dimensional (2-DG) gel analysis of cochlear proteins was published [30]. We have now extended this mapping proteomics approach to the central auditory system in order to characterize protein profiles and to identify proteins in the SOC and the IC. Differential centrifugation yielded four different protein fractions each. The 2-DG protein patterns of corresponding fractions were compared with each other and with that of the cerebellum. This may allow the detection of proteins specific to an auditory region. For protein identification, 50 protein spots of the cytosolic SOC fraction and 11 spots from the corresponding IC fraction were subsequently analysed by mass spectrometry. These and forthcoming proteomics data are part of an integrated database of the gene repertoire of the auditory brainstem (ID-GRAB), that is publicly available (http://www.id-grab.de).

2. Materials and methods

2.1. Materials

Immobilized pH gradient (IPG) strips and carrier ampholytes were purchased from Amersham Biosciences (Heidelberg, Germany). Acrylamide and the other reagents for polyacrylamide gel preparation as well as most other chemicals were from Roth (Karlsruhe, Germany). SB3–10 was supplied by Sigma (München, Germany) and the protease inhibitor cocktail by Roche (Mannheim, Germany). Antibody 20E8 against cytochrome oxidase IV was purchased from Molecular Probes (Göttingen, Germany), anti-GM130 from BD Transduction Laboratories (Heidelberg, Germany), anti-Hht1-C was a gift of G. Schlenstedt (Heidelberg, Germany), and a5 against the Na^+/K^+-ATPase was obtained from the Developmental Studies Hybridoma Bank of the University of Iowa (Iowa, USA).

2.2. Animals

Sprague–Dawley rats of both genders (8–9 weeks old) were deeply anaesthetised by a peritoneal injection of 500 mg/kg ketamine and sacrificed by decapitation. All protocols complied with the current German Animal Protection Law and were approved by the local animal care and use committee (Landesuntersuchungsamt Koblenz). The cerebellum was separated from the brainstem by cutting horizontally through its pedunculi and the IC was excised from the brainstem. The SOC area was excised bilaterally under visual control from 400-μm thick transverse brainstem slices using the lateral and dorsal boundaries of the LSO as hallmarks. Tissue samples were immediately frozen in liquid nitrogen.

2.3. Sample preparation and separation

For the SOC, samples from eight animals of both genders were pooled. Likewise, samples from four animals were pooled for the IC and the cerebellum. Brain samples were resuspended in 2–3.5 ml of homogenisation buffer (20 mM HEPES-OH, pH 7.5, 320 mM sucrose, 1 mM EDTA, 5 mM DTT, 1 mM PMSF, 1 mM sodium vanadate, 1 mM sodium fluoride and a protease inhibitor cocktail (Complete™), 1 tablet per 50 ml). The tissue samples were homogenised on ice by applying thirty strokes in a glass homogeniser. Fractionation of the suspensions was performed using a protocol previously established to analyse brain proteins [21]. In short, samples were centrifuged at 800 *g* for 10 min to sediment nuclei and cell debris. The supernatant was centrifuged again at 10 000 *g* for 15 min to obtain the mitochondrial pellet. The corresponding supernatant was centrifuged again at 100 000 *g* for 1 h to yield the microsomal pellet, and the cytosolic supernatant which was used without change for 2-DGE. The 800 *g* pellet was resuspended in 7 M urea, 2 M thiourea, 2% CHAPS, 40 mM Tris, cleaned up by precipitation using the 2-D clean up kit (Amersham Biosciences, Freiburg, Germany), and dissolved in rehydration buffer (5 M urea, 2 M thiourea, 2% CHAPS, 2% SB 3–10 and 40 mM Tris) prior to 2-DGE. For the cytosolic fraction, the protein concentration was determined using a micro BCA assay (Pierce, Bonn, Germany), for the 800 *g* pellet P1 (resuspended in a thiourea containing buffer), the protein amount was quantified by comparing in a 12% 1-D SDS–PAGE a dilution series with an 800 *g* pellet P1 previously

resuspended in phosphate buffer and quantified with the micro-BCA assay. For analytical gels, 200 μg protein, and for preparative gels, 500 μg protein were applied to 18-cm long IPG strips (pH 3–10) and isoelectric focusing was performed for 40 000 Vh on an IPGphor (Amersham Biosciences). After equilibration, the gel strips were transferred to a 12% SDS–PAGE in the second dimension using a Protean II xi cell (Bio-Rad, München, Germany). Analytical gels were stained with a modified silver staining protocol that lacks glutaraldehyde and that was reported to be compatible with in-gel digestion and mass spectrometry analysis [29]. Preparative gels were stained with colloidal Coomassie blue G250 (17% ammonium sulfate, 34% methanol, 0,55 acetic acid, 0,1% Coomassie blue G250) for 3–5 days. For analytic gels, three gels were run for each fraction obtained from the SOC and the IC, and two gels for fractions of the cerebellum; for preparative gels, two gels were performed for each fraction. Judged from visual inspection, the reproducibility between the different gels of a same sample fraction was rather good. Differences were assessed by visual judgement of the protein spots. Spot counts were performed using AnalySIS (version 3.0, SIS, Münster, Germany). Each gel was scored five times and the mean value and the standard deviations were calculated.

2.4. Immunoblot analysis

A 20-μg portion of protein of each fraction was resolved by SDS–PAGE using either an 8% or a 12% Laemmli system. Proteins were electrophoretically transferred to PVDF membranes for 2 h at 1 mA/cm^2 membrane surface using a semidry blotter (Peqlab, Erlangen, Germany). PVDF-bound proteins were visualized by staining with Poinceau S, then blocked in TTBS–milk [20 mM Tris (pH 7.5), 150 mM NaCl, 0,1% Tween-20, 5% nonfat dry milk] for 1 h and subsequently incubated in the same buffer with the respective antiserum overnight at 4 °C. Antibodies were directed against the following marker proteins: anti-Hht1-C against histone H3 (cell nucleus), anti-COX IV against cytochrome oxidase subunit IV (mitochondria), anti-GM130 against Golgi matrix protein of 130 kDa (Golgi complex), and a5 against the α1 subunit of the Na^+/K^+-ATPase (plasma membrane). After four washes in TTBS, the secondary antibody (horseradish peroxidase-conjugated goat anti-rabbit or anti-mouse IgG (1:5000, Amersham Biosciences, Heidelberg, Germany) was applied for 1 h. After four washes in TTBS, bound antibody was detected using an enhanced chemiluminescence assay (Amersham Biosciences) and exposure to an X-ray film RX (Kisker, Steinfurt, Germany).

2.5. Protein identification by mass spectrometry

Protein spots were manually excised from the gel, washed, and in-gel digested using the Montage in-gel Digest96 kit (Millipore, Eschborn, Germany) following the manufacturer's instruction. The sample was desalted using μC_{18}-Ziptips (Millipore), and the eluent was loaded into a nanoelectrospray capillary (Waters Micromass, Manchester, UK). All measurements were performed in a tandem mass spectrometer (Q-Tof 2, Waters Micromass) equipped with an electrospray source. To determine peptide sequences, tandem mass spectrometry was performed by selecting precursor ions using the quadrupole. Peptides were fragmented in the collision chamber using energies between 20 and 40 eV and argon as the collision gas. Peptide fragments were detected by the TOF analyser. Data acquisition and processing were performed using the MASSLYNX 3.5 software package (Waters Micromass). The resultant peptide sequences were submitted to a BLAST search for short and nearly exact matches using NCBI's nonredundant (nr) database (http://www.ncbi.nlm.nih.gov/BLAST/).

Both the relative molecular weight (M_r) and the isoelectric point (p*I*) of the intact protein, as judged from the 2-DGs, were used as further criteria for protein identification. For most of the identified proteins, two to four tryptic peptides were matched by mass and sequence to the top candidates retrieved by the searches. No second-pass searches were performed to identify any less abundant proteins that might co-migrate with the major proteins. To classify identified proteins, functional information was retrieved mainly from the Swiss-Prot database (http://us.expasy.org/sprot/).

3. Results

3.1. Fractionation of the tissue sample and immunoblot analysis

As a first step towards a global analysis of the protein content in identified regions of the mammalian auditory brainstem, SOC and IC were isolated from 8–9-week-old rats of both genders and pooled in order to minimise differences between individual animals. In addition, the cerebellum, as a nonauditory structure, was subjected to the same analysis. As brain tissues are likely to possess a highly complex protein content, samples were fractionated by differential centrifugation in order to obtain a reduced complexity prior to 2-DG separation.

To characterize the subcellular composition of the fractions obtained after differential centrifugation, immunoblot analyses were performed with antibodies against marker proteins for the cell nucleus, the endoplasmic reticulum (ER), the Golgi complex, the plasma membrane, and for mitochondria (Fig. 1). These analyses revealed that the 800 *g* pellet P1 contained proteins of most of these subcellular compartments (nuclei, Golgi complex, plasma membrane, and mitochondria). Only the marker protein for ER was not detected in this fraction. This is in agreement

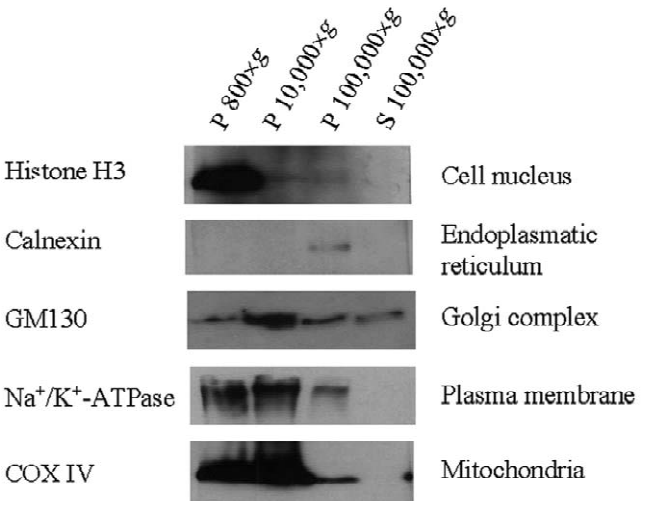

Fig. 1. Immunoblot analysis of the fractionation procedure via differential centrifugation. After homogenisation of cerebellar samples, three rounds of consecutive centrifugation with increasing *g* values were performed. A 20-μg amount of each of the resulting four fractions (800 *g*, 10 000 *g*, 100 000 *g* pellets, and 100 000 *g* supernatant) were separated by one-dimensional SDS–PAGE and transferred to a membrane. Each fraction was analysed with compartment-specific antibodies: anti-histone H3 (cell nucleus), anti-Calnexin (endoplasmic reticulum), anti-GM130 (Golgi complex), anti-Na^+/K^+-ATPase (plasma membrane), and anti-cytochrome oxidase IV (mitochondria). Antibodies are indicated on the left, compartment specificity is indicated on the right. Fractions are indicated above the blots (P = pellet; S = supernatant). The results indicate an enrichment of the endoplasmic reticulum in the 100 000 *g* pellet and a relatively pure cytosolic (100 000 *g* supernatant) fraction.

with the fact that nuclei and large membrane sheets, as well as undissolved material such as cell debris and entire cells, sediment at 800 *g*. The 10 000 *g* pellet was enriched for the Golgi complex, yet it also contained mitochondria and plasma membranes. The ER appeared to be present exclusively in the 100 000 *g* microsomal pellet. However, due to the weak signal of the antibody in the ER fraction, which indicates a weak binding, a faint presence of ER in other fractions cannot be excluded. In the post 100 000 *g* supernatant, a faint signal was obtained only with the marker for the Golgi complex. Thus, this fraction mainly contains cytosolic proteins. Taken together, these data are in agreement with a previous mass spectrometric analysis showing an enrichment of mitochondrial proteins in the 10 000 *g* pellet and of cytosolic proteins in the final supernatant [21].

3.2. Analytical two-dimensional gel electrophoresis

According to our immunoblot analysis, proteins that may confer specificity to neurons, such as signalling proteins, transcription factors, and plasma membrane proteins, were enriched in the 800 *g* pellet and the post 100 000 *g* supernatant. Therefore, the protein content of these two fractions was separated by 2-DGE and the protein spots were visualized by silver staining. Within the limitation of our method (i.e. visual inspection) to compare gels, the reproducibility between different gels of the same sample was rather good. Representative examples of the separation are shown in Figs. 2 and 3. The overall spot patterns obtained from the SOC, the IC, and the cerebellum were similar for a given fraction. However, a closer inspection revealed noteworthy differences between the three tissues. Examples are illustrated by the circled areas in Figs. 2 and 3. At a higher magnification of the 2-DGs obtained from the cytosolic fractions, it became evident that these differences encompass both the expression level (rectangular areas in Fig. 4) and number of isoforms present (circled areas in Fig. 4). In the upper acidic part of the gels, for instance, two proteins are weakly present in the SOC, scarcely detectable in the IC, yet abundant in the cerebellum (Fig. 4; rectangular areas). In the lower part, a cluster of five (IC and cerebellum) and six (SOC) proteins is visible. Sequence analysis of the corresponding spots from Coomassie-stained gels identified isoforms of phosphatidylethanolamine-binding protein (= Raf-kinase inhibitor protein 1; Fig. 5A; spots 1–4). Most of the differences observed at higher magnification relate to low- and medium-abundance proteins. This complicates their assessment in an entire 2-DG which requires more sophisticated tools than visual inspection. Therefore, no estimate was made concerning the total number of differences between the three tissues.

Visual inspection of the 2-DGs obtained from the 800 *g* pellets yielded 674±59 spots in the SOC, 456±66 in the IC, and 485±26 in the cerebellum (Table 1). Likewise, the cytosolic fraction yielded 568±68 spots in the SOC, 559±30 in the IC, and 656±53 in the cerebellum (Table 1). These numbers represent a conservative score because only clearly visible and distinct protein spots were counted. Due to the highly dynamic range of protein abundance [5,18], some gel areas, such as the high-molecular weight area in the acidic part, are clearly overloaded (arrows in Figs. 2 and 3). Zooming-in on these areas with narrow-range pH gradients in the first dimension will likely reveal many more distinct protein spots [36].

3.3. Identification of high-abundance cytosolic proteins of the SOC by mass spectrometry

In order to identify the high-abundance proteins in the SOC and the IC, preparative 2-DGs of the cytosolic

Fig. 2. Two-dimensional gels of 800 *g* pellets. A 200-μg amount of the 800 *g* pellets (A, SOC; B, IC; C, cerebellum) was separated in the first dimension on an 18-cm IEF strip (pH 3–10) and in the second dimension by 12% SDS–PAGE. Proteins were visualized by silver staining. Relative molecular masses (M_r) are indicated on the left, the orientation of the pH gradient is depicted above the gels. Circled areas indicate examples of notable differences between the three tissues, arrows illustrate overloaded areas. All three tissues displayed similar patterns of high-abundance spots, but an increased spot number is evident in the SOC fraction.

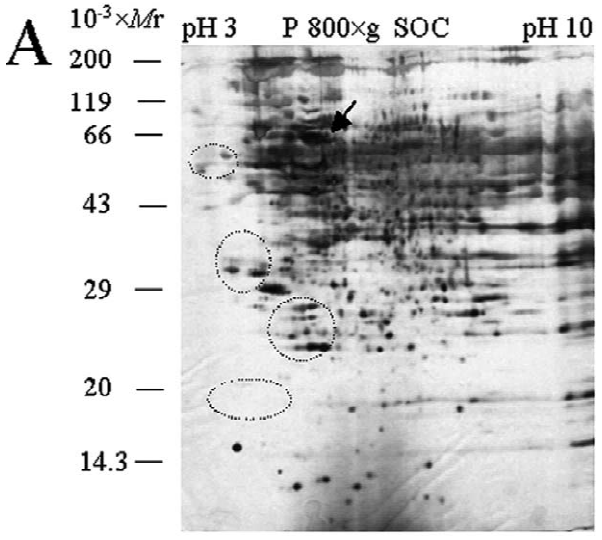
A
$10^{-3}\times Mr$
pH 3
P 800×g SOC
pH 10
200
119
66
43
29
20
14.3

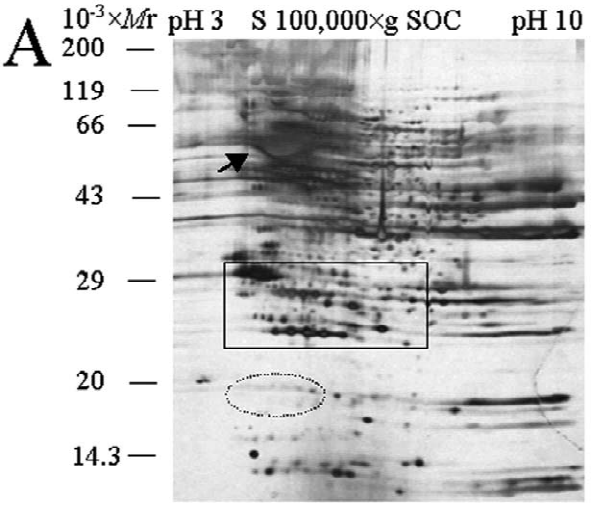
A
$10^{-3}\times Mr$
pH 3
S 100,000×g SOC
pH 10
200
119
66
43
29
20
14.3

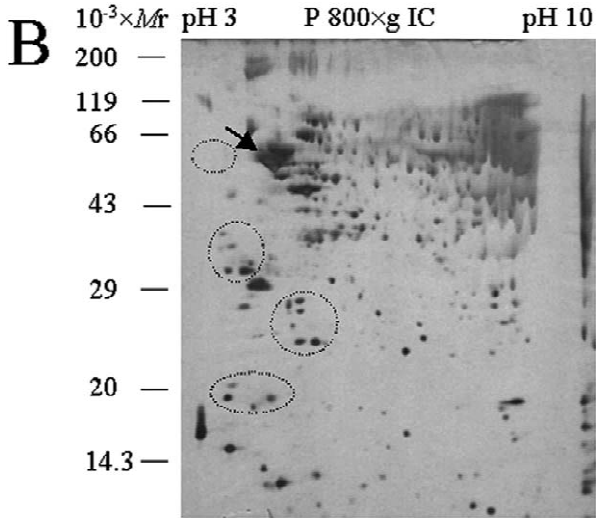
B
$10^{-3}\times Mr$
pH 3
P 800×g IC
pH 10
200
119
66
43
29
20
14.3

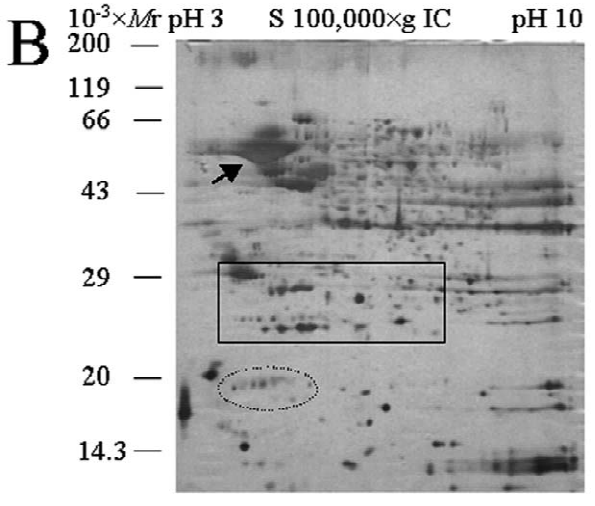
B
$10^{-3}\times Mr$
pH 3
S 100,000×g IC
pH 10
200
119
66
43
29
20
14.3

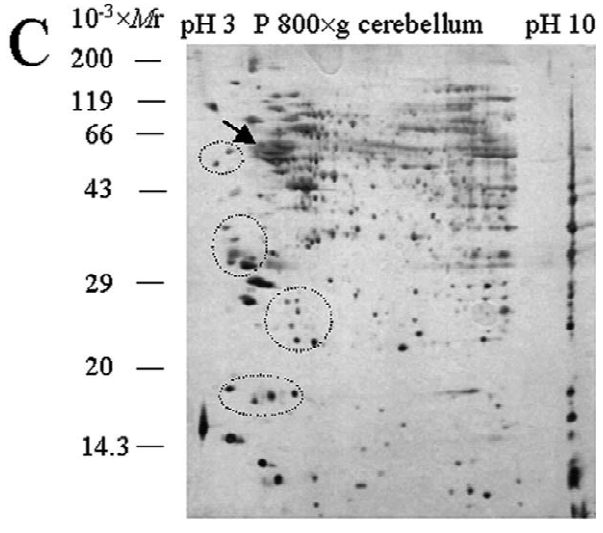
C
$10^{-3}\times Mr$
pH 3
P 800×g cerebellum
pH 10
200
119
66
43
29
20
14.3

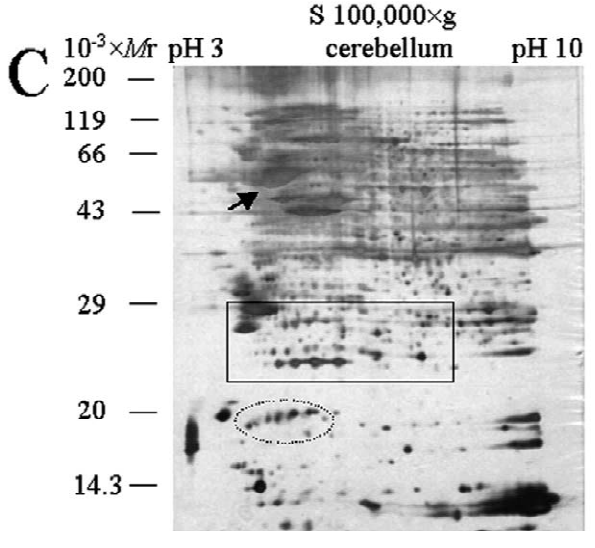
C
$10^{-3}\times Mr$
pH 3
S 100,000×g
cerebellum
pH 10
200
119
66
43
29
20
14.3

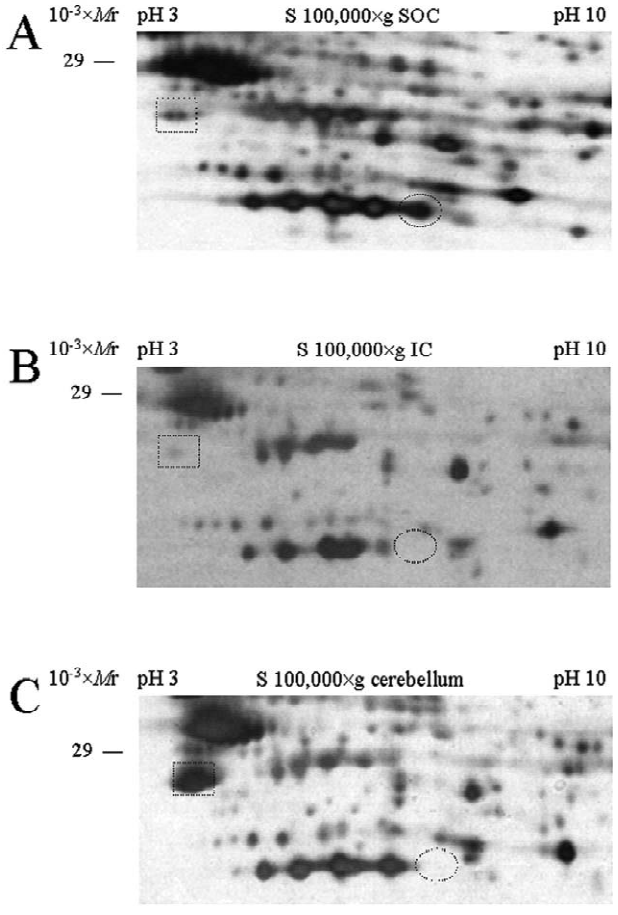

Fig. 4. Enlarged two-dimensional gel images of 100 000 *g* supernatants. Images depict the rectangular areas marked in Fig. 3 on the 2-DGs of the 100 000 *g* supernatants (A, SOC; B, IC; C, cerebellum). Circled areas indicate a variation in number of isoforms between the three tissues. Rectangular areas indicate a difference in spot intensity between the three tissues. Relative molecular masses (M_r) are indicated on the left, the orientation of the pH gradient is depicted above the gels. Differences between the three tissues are mainly restricted to spots of low to medium intensity.

fractions of these two tissues were performed. The cytosolic fraction was chosen, because it was the purest subcellular compartment obtained by our fractionation protocol. Initial experiments using silver-stained protein spots yielded poor mass spectrometric data. Therefore, gels were stained with colloidal Coomassie blue (Fig. 5). Close

Fig. 3. Two-dimensional gels of 100 000 *g* supernatants. A 200 μg amount of the 100 000 *g* supernatants (A, SOC; B, IC; C, cerebellum) was separated in the first dimension on a 18 cm IEF strip (pH 3–10) and in the second dimension by 12% SDS–PAGE. Proteins were visualized by silver staining. Relative molecular masses (M_r) are indicated on the left, the orientation of the pH gradient is depicted above the gels. The circled area indicates an example of notable differences between the three tissues, the solid rectangles indicate the areas shown at higher magnification in Fig. 4, arrows illustrate overloaded areas. All three tissues displayed a similar spot pattern.

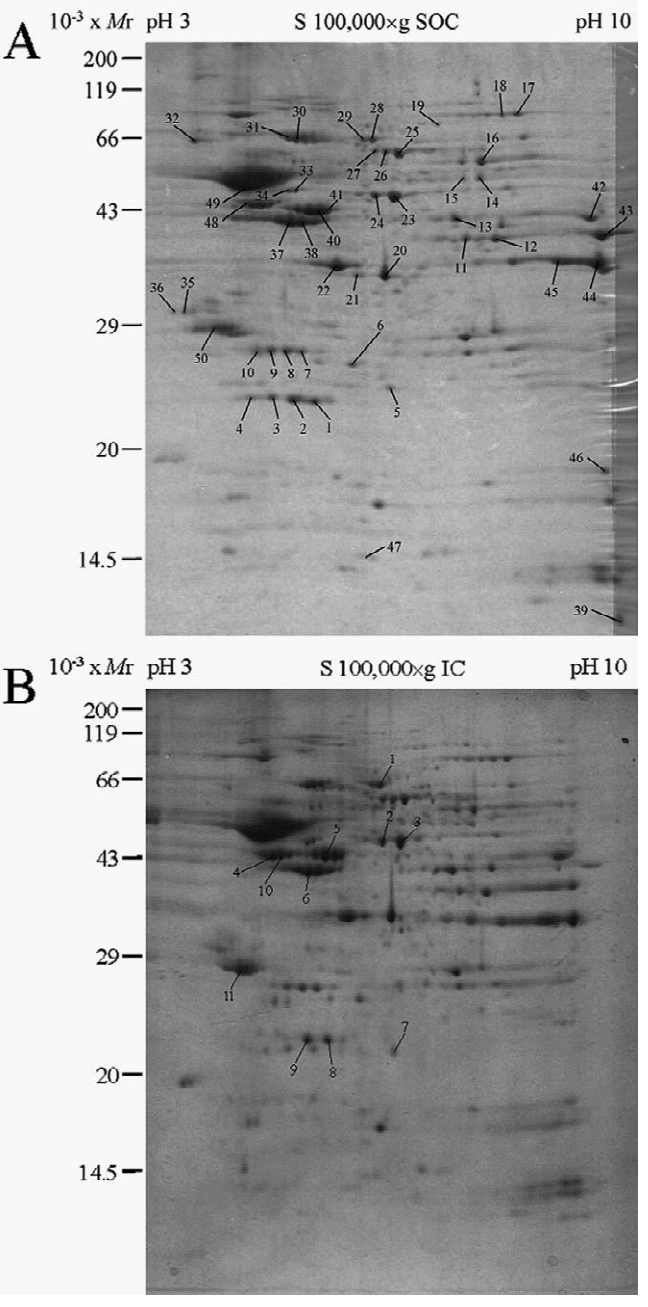

Fig. 5. Preparative two-dimensional gels of the 100 000 *g* supernatants of SOC and IC. A 500-μg amount of 100 000 *g* supernatants (A, SOC; B, IC) were separated in the first dimension on an 18-cm IEF strip (pH 3–10) and in the second dimension by 12% SDS–PAGE. Proteins were visualized by colloidal Coomassie staining. Relative molecular masses (M_r) are indicated on the left, the orientation of the pH gradient is depicted above the gels. Numbered protein spots were identified by mass spectrometry and are listed in Tables 2 and 3. Proteins 1–11 in (B) are identical to proteins at equivalent positions in (A).

to 300 protein spots were detected in the extracts of the two tissues (Table 1), roughly half the amount detected with the more sensitive silver staining protocol. In contrast to results obtained with the more sensitive silver staining

Table 1
Protein spot count

	Subcellular fraction		
	Superior olivary complex	Inferior colliculus	Cerebellum
800 *g* pellet[a]	674±59	456±66	485±26
100 000 *g* supernatant[a]	568±68	559±30	656±53
100 000 *g* supernatant[b]	278±12	293±26	N.d.

The table lists the mean number of spots on respective 2-DG as determined by manual enumeration. Values represent mean±standard deviation of five counts.
[a] Numbers derived from silver-stained gels.
[b] Numbers derived from colloidal Coomassie blue G250-stained gels.

protocol (Fig. 3), the protein expression pattern achieved upon colloidal Coomassie blue staining revealed only few differences between these two auditory structures (Fig. 5). This is in agreement with the notion that most differences are due to low- and medium-abundance proteins. Due to the high degree of concord in the 2-DG patterns, mainly protein spots of the SOC cytosolic fraction were analysed by mass spectrometry. This resulted in the identification of 50 proteins, encoded by 30 independent genes (Table 2). Fifteen proteins were present in two or more isoforms. For example, the phosphatidylethanolamine-binding protein and the Rho GDP-dissociation inhibitor 1 were detected in four different isoforms with almost identical molecular masses. In total, twelve proteins (40%) were detected in two isoforms, one (3%) in three isoforms, two (7%) in four isoforms. All of the isoforms differed in p*I*, whereas no major shift was observed in molecular mass (Tables 2 and 3). Most isoforms showed a p*I* difference of 0.1–0.3, the only marked exception were two glyceraldehyde-3-phosphate dehydrogenase isoforms with a p*I* difference of 0.8.

According to information available in the databases, the majority of identified proteins (21/30) were of cytoplasmic origin or attributed as such due to sequence similarities with known cytoplasmic proteins (Table 2). For seven proteins, the subcellular localization has not yet been elucidated (Table 2). The database information confirms the enrichment for cytosolic proteins achieved by our fractionation method. The identification of two mitochondrial proteins, however, indicates a mild contamination of the cytosolic fraction with mitochondrial matter.

To assess whether the high degree of similarity between the cytosolic spot patterns obtained from SOC and IC is indeed due to the expression of identical proteins, eleven spots of equivalent position in the IC 2-DG were identified as well (Table 3). Sequence analysis showed that all eleven IC spots contained the same protein as in the equivalent position of the SOC 2-DG (Tables 2 and 3). This demonstrates that the similarity in the overall spot pattern between the SOC and IC reflects a true concord on the level of major proteins.

4. Discussion

A catalogue at high spatial and temporal resolution of the expressed genes in various regions of the nervous system will be a powerful resource for understanding brain development and function. Several neuroproteome studies have been initiated recently. These included the analysis of the entire brain in the rat [6,9,21] and the mouse [2,20], the mouse cerebrum [31,32] and cerebellum [1], and the human parietal cortex [22]. To contribute to such a 'parts list', we initiated a project which is aimed at the large-scale analysis of the molecular machinery underlying neural structure and function, and the development of different processing centres in the auditory brainstem. The auditory brainstem was chosen because it displays several interesting features, such as an exquisite topographical (tonotopical) organization [17,19] and unique properties of temporally accurate information processing in the submillisecond range [33,34].

In this paper, we present the first data of our proteomics approach on the SOC, the IC, and the cerebellum. The latter brain structure was analysed to allow a comparison between the auditory structures and a nonauditory structure. Our 2-DGE analysis focused on the most interesting two subcellular fractions with respect to neuronal functioning, namely the 800 *g* pellet with the enrichment for nuclear and plasma membrane proteins, and the cytosolic fraction. The former contains transcription factors, receptors and channels, whereas the latter contains proteins of the signalling pathways and those contributing to the cytoarchitecture. The 10 000 *g* and 100 000 *g* pellets were not analysed in the present study as we assume that there is only a minor contribution of the mitochondrial proteome and of the proteins of the secretory pathway (Golgi complex and ER) to the specific tasks of a given neuronal tissue. For a given subcellular fraction, the overall pattern of the abundant proteins was similar between the three tissues. Whereas the spot count for the cytosolic fraction was also rather similar for all three fractions, especially between SOC and IC (568 versus 559), the 800 *g* pellet obtained from the SOC yielded roughly 40% more spots than those from the IC and the cerebellum. This higher number was mainly attributable to proteins with a M_r >25 000. As the 800 *g* pellet contained several subcellular compartments, such as the cell nucleus and the plasma membrane, it is unclear whether this reflects a general increase in protein complexity of the SOC compared to the IC or whether it can be ascribed to a specific subcellular compartment. The latter is suggested by the fact that the cytosolic fractions of the SOC and the IC displayed a very similar spot number. A clarification of this issue requires improved subcellular fractionation protocols.

According to our immunoblot analysis, the cytosolic fraction represented the purest subcellular compartment. As information on subcellular localization is important for a functional assessment, we identified protein spots of the

Table 2
Proteins of the cytosolic fraction from the rat SOC

		Acc. no. (NCBI)	Acc. no. (Swiss-Prot)	Theoretical $M_r \times 10^{-3}/pI$	Observed $M_r \times 10^{-3}/pI$	Subcellular localization
1	Phosphatidylethanolamine-binding protein[S]	NP_058932	P31044	21/5.7	22/6.0	Cytosolic
2	Phosphatidylethanolamine binding protein[S]	NP_058932		21/5.7	21/5.7	Cytosolic
3	Phosphatidylethanolamine binding protein[S]	NP_058932	P31044	21/5.7	21/5.4	Cytosolic
4	Phosphatidylethanolamine binding protein[S]	NP_058932	P31044	21/5.7	21/5.1	Cytosolic
5	Contraception associated protein 1[X]	CAA07434	O88767	20/6.7	23/7	Unknown
6	Thiol-specific antioxidant protein[X]		O88433	25/5.8	25/6.5	Cytosolic
7	Rho GDP-dissociation inhibitor 1[S]	Q99PT1[1]	Q99PT1[1]	23/5.2	26/6	Cytosolic
8	Rho GDP-dissociation inhibitor 1[S]	Q99PT1[1]	Q99PT1[1]	23/5.2	26/5.6	Cytosolic
9	Rho GDP-dissociation inhibitor 1[S]	Q99PT1[1]	Q99PT1[1]	23/5.2	26/5.4	Cytosolic
10	Rho GDP-dissociation inhibitor 1[S]	Q99PT1[1]	Q99PT1[1]	23/5.2	26/5.2	Cytosolic
11	Fructose-bisphosphate aldolase[M]	ADRTC	P05065	39/7.1	38/8.0	Cytosolic
12	Fructose-bisphosphate aldolase[M]	ADRTC	P05065	39/7.1	38/8.4	Cytosolic
13	Glutamine synthetase[M]	NP_058769	P09606	42/7.3	42/7.9	Cytosolic
14	Glutamate dehydrogenase[M]	NP_036702	P10860	61/8.3	50/8.2	Mitochondrial
15	Glutamate dehydrogenase[M]	NP_036702	P10860	61/8.3	50/8.0	Mitochondrial
16	Pyruvate kinase[M]	NP_445749	P11981	58/7.0	54/8.2	Cytosolic
17	Mitochondrial aconitase[M]	NP_077374	Q9ER34	85/8.1	87/8.7	Mitochondrial
18	Mitochondrial aconitase[M]	NP_077374	Q9ER34	85/8.1	87/8.5	Mitochondrial
19	*N*-etyhlmaleimide sensitive factor[X]		O88960	83/6.9	73/7.7	Unknown
20	Malate dehydrogenase-like enzyme[M]	NP_150238	MDHM_*R*[2]	36/6.5	34/6.9	Cytosolic
21	Malate dehydrogenase-like enzyme[M]	NP_150238	MDHM_*R*[2]	36/6.5	34/6.6	Cytosolic
22	Lactate dehydrogenase B[M]		P42123	37/6.0	34/6.3	Cytosolic
23	Alpha enolase[M]	P04764	P04764	47/6.1	45/7.0	Cytosolic
24	Alpha enolase[M]	P04764	P04764	47/6.1	45/6.8	Cytosolic
25	Dihydropyrimidinase related protein-2[N]	P47942	P47942	62/7.2	56/7.1	Cytosolic
26	Dihydropyrimidinase related protein-2[N]	P47942	P47942	62/7.2	56/7.0	Cytosolic
27	Dihydropyrimidinase related protein-2[N]	P47942	P47942	62/7.2	62/6.8	Cytosolic
28	Albumin[M]	NP_599153	Q63036[3]	69/6.4	66/6.8	Secreted
29	Albumin[M]	NP_599153	Q63036[3]	69/6.4	66/6.7	Secreted
30	Heat shock protein 70-1[X]	NP_114177	Q07439	70/5.6	64/5.8	Cytosolic
31	Heat shock protein 70-1[X]	NP_114177	Q07439	70/5.6	64/5.6	Cytosolic
32	Neurofilament, light polypeptide[N]	NP_113971	P19527	61//4.7	63/4.4	Unknown
33	Glial fibrillary acidic protein α[N]	AAD01873	Q9R1Q[3]	50/5.5	46/5.8	Unknown
34	Glial fibrillary acidic protein α[N]	AAD01873	Q9R1Q[3]	50/5.5	46/5.6	Unknown
35	Tyrosin 3-monooxygenase[N]	NP_113791	P04177	29/4.6	30/4.3	Unknown
36	Tyrosin 3-monooxygenase[N]	NP_113791	P04177	29/4.6	30/4.1	Unknown
37	Actin, gamma[C]	S11222	P02571	42/5.4	40/5.7	Cytosolic
38	Actin, gamma[C]	S11222	P02571	42/5.4	40/5.8	Cytosolic
39	Diazepam binding inhibitor[N]	NP_114054	P11030	10/9.1	10/9.9	Cytosolic
40	Creatine kinase-B[M]		P07335	43/5.5	42/6.1	Cytosolic
41	Creatine kinase-B[M]	AAA40930		43/5.5	42/6.2	Cytosolic
42	Phosphoglycerate kinase 1[M]	NP_445743	P00558[4]	45/8.0	41/9.7	Cytosolic
43	Aldolase A, fructose bisphosphate[M]	NP_036627	P05065	39/8.5	38/9.8	Cytosolic
44	Glyceraldehyde-3-phosphate dehydrogenase[M]	DERTG	Q8K4T7[3]	36/8.6	34/9.8	Cytosolic
45	Glyceraldehyde-3-phosphate dehydrogenase[M]	DERTG	Q8K4T7[3]	36/8.6	34/9.0	Cytosolic
46	Cofilin 1[C]		P45592	19/8.5	17/9.8	Cytosolic
47	Profilin IIa[C]	Q9EPC6	Q9EPC6		10/7.4	Unknown
48	Gamma enolase[M]	P07323	P07323	47/5.1	44/5.3	Cytosolic
49	Similar to tubulin, β, 2[C]	XP_216012	Q8VIP3[3]	50/4.8	47/5.0	Cytosolic
50	Tyrosin 3-monooxygenase[N]	NP_037143	P04177		28/7.0	Unknown

Spot no. corresponds to the position marked on the gel (Fig. 5A), protein name and Acc. no. (NCBI) are derived from the NCBI database (http://www.ncbi.nlm.nih.gov/BLAST/), and Acc. no. (Swiss-Prot) relates to the Swiss-Prot protein knowledge base (http://us.expasy.org/sprot/). Superscript letters indicate protein function as categorized in Table 4: [M], Basic metabolism and cell function; [C], cytoarchitecture; [S], signal transduction; [B], brain-specific function; [X], other function or not annotated. Theoretical M_r/pI was calculated from the amino acid sequence, and observed M_r/pI was derived from the spot's position in the gel. Information on subcellular localization was taken from the Swiss-Prot protein knowledge base. [1], Databank entry relates to the mouse protein; [2], Subcellular localisation is conferred from the malate dehydrogenase; [3], Swiss-Prot entry for this protein lists only partial sequence, full length entries exist for other species; [4], Swiss-Prot entry for this protein is derived from human but listed as identical to rat.

Table 3
Proteins of the cytosolic fraction from the rat IC

Spot no.	Protein name	Acc. no. (NCBI)	Acc. no. (Swiss-Prot)	Theoretical $M_r \times 10^{-3}$/pI	Observed $M_r \times 10^{-3}$/pI	Subcellular localization
1	Albumin[M]	NP_599153	Q63036[1]	69/6.4	61/6.5	Secreted
2	Alpha enolase[M]	P04764	P04764	47/6.1	46/6.5	Cytosolic
3	Alpha enolase[M]	P04764	P04764	47/6.1	46/6.7	Cytosolic
4	Gamma enolase[M]	P07323	P07323	47/5.1	43/5.0	Cytosolic
5	Creatine kinase-B[M]	AAA40933	P07335	40/6.1	43/5.7	Cytosolic
6	Actin, gamma[C]	S11222	P02571	42/5.4	40/5.5	Cytosolic
7	Thiol-specific antioxidant protein[X]		O88433	25/5.8	24/6.2	Cytosolic
8	Phosphatidylethanolamine-binding protein[S]	NP_058932	P31044	21/5.7	22/5.7	Cytosolic
9	Phosphatidylethanolamine-binding protein[S]	NP_058932	P31044	21/5.7	22/5.5	Cytosolic
10	Gamma enolase[M]	P07323	P07323	47/5.1	43/5.1	Cytosolic
11	Tyrosin 3-monooxygenase[N]	NP_037143	P04177		27/4.6	Unknown

Spot no. corresponds to the position marked on the gel (Fig. 5B), protein name and Acc. no. (NCBI) are derived from the NCBI database (http://www.ncbi.nlm.nih.gov/BLAST/), and Acc. no. (Swiss-Prot) relates to the Swiss-Prot protein knowledge base (http://us.expasy.org/sprot/). Superscript letters indicate protein function as categorized in Table 4: [M], Basic metabolism and cell function; [C], cytoarchitecture; [S], signal transduction; [B], brain-specific function; [X], other function or not annotated. Theoretical M_r/pI was calculated from the amino acid sequence, and observed M_r/pI was derived from the spot's position in the gel. Information on subcellular localization was taken from the Swiss-Prot protein knowledge base. [1], Swiss-Prot entry for this protein list only partial sequence. Full length entries exist for other species.

cytosolic SOC fraction by mass spectrometry. Our mass spectrometry data confirmed the cytosolic origin of the fraction and, thus, the purity of the sample. A total of 28 out of 30 (93%) identified proteins are compatible with a cytosolic localisation. The remaining two proteins were of mitochondrial origin. This contamination is possibly due to a disintegration of the organelle during the homogenisation procedure. Sequencing of eleven spots at equivalent positions in the SOC and IC 2-DGs demonstrated identity for each corresponding spot between the two auditory centres. This shows that the observed similarity in the overall protein pattern between SOC and IC is indeed due to identical proteins.

The 30 proteins identified in the cytosolic 2-DGs can be grouped into five broad functional categories (Table 4). With 14 members, enzymes involved in basic cell metabolism, especially the glycolytic cycle, such as pyruvate kinase or aldolase A, represent the largest group. Together with the identified structural proteins (actin, gamma; protein similar to tubulin β 2), these are housekeeping proteins expected to be present in every cell type and in high copy numbers. In addition, we identified two proteins (phosphatidylethanolamine-binding protein; Rho GDP-dissociation inhibitor 1) involved in signal transduction pathways. Interestingly, these were present in four isoforms whereas proteins of the other categories were detected in no more than three isoforms. This indicates that post-translational modifications play a significant role in their function. The shift in the pI values of these proteins within a range of 0.1–0.3, without an apparent change in M_r, is in accordance with low molecular-mass modifications, such as phosphorylation, that mainly affect protein net charge. Finally, six brain-specific proteins were identified. They included widely known molecular markers for neuronal and glial cells (neurofilament light polypeptide; glial fibrillary acidic protein α) but also less common proteins (tyrosin 3-monooxygenase; dihydropyrimidinase related protein-2). The former plays an important role in the physiology of adrenergic neurons [14], and for the latter, a function in axon elaboration has been postulated [26]. In total, for half of the identified proteins (15/30), isoforms were identified. This confirms previous notions that post-translational modifications play important roles in higher eucaryotes [25]. Furthermore, it underlines the need

Table 4
Functions of the identified cytosolic SOC proteins

Protein function		Number of spots identified	Corresponding number of genes
Basic metabolism/cell function	M	22	14
Cytoarchitecture	C	5	4
Signal transduction	S	8	2
Brain-specific	B	10	6
Other (or not annotated)	X	5	4
Total		50	30

The table represents a classification into five broad categories, based on known or postulated protein functions. Symbol denotes the one-letter code used to identify the corresponding protein function for each protein in Tables 2 and 3. Number of spots pertains to total number of spots identified belonging to a given category, whereas number of genes lists the number of different genes identified, without consideration of possible isoforms.

for large-scale analysis on the protein level to fully identify the protein repertoire in a given brain region, as this increase in complexity is not amenable to expression analysis on the nucleic acid level and not predictable from protein sequences alone.

So far, our list does not include any cytosolic proteins known to be highly present in the mammalian auditory brainstem centres, such as the calcium binding proteins calbindin, parvalbumin, or calretinin [10,23]. An explanation of this finding is that the SOC contains numerous types of neuronal and non-neuronal cells. Whereas the concentration of ubiquitous housekeeping proteins is independent of the number of cell types present, the concentration of proteins that differ between cell types will decrease as the complexity of the sample increases. For instance, in the SOC of adult rats, parvalbumin is expressed only in the MNTB [23] and, therefore, its detection will be difficult in a complete SOC protein extract. This explanation is supported by the fact that 27 out of 50 (54%) identified spots represented housekeeping proteins (Table 4) and by the finding that differences in the 2-DGs were mainly restricted to low- to medium-abundance protein spots. As a consequence, a reduction in sample complexity is necessary for brain proteomics approaches to detect proteins conferring specific functions to a neuronal network. This is especially mandatory for neuroproteomics, as the brain is the most complex organ. Along that line, a recent analysis of 161 genes from mouse chromosome 21 revealed that 85% of them are expressed in the adult brain, but only 21% in muscles [28].

We adopted the strategy of subcellular fractionation to reduce sample complexity without loosing the essential information on the intracellular localisation of the identified proteins, since the latter is crucial for functional annotations. However, for future, in-depth analyses of the auditory brainstem, further methodological refinements will be necessary. Important subcellular compartments, such as the plasma membrane, could not be isolated and purified. This is likely due to the fact that only simple differential centrifugation was performed. More elaborate subcellular fractionation protocols exist and are being improved, but the increased amount of required starting material mandates their assessment before they can be applied to small tissue amounts. We are currently developing a single tube protocol to separate nuclei, membranes, and cytosol in a first step and, in a second step, to further separate the membrane fraction into ER, Golgi complex and plasma membrane on a single nycodenz gradient.

Even in cases where the protocol used in the present study yielded a rather pure fraction (such as the cytosol), the complexity of the sample remained very high. This fact, in combination with the highly dynamic range of proteins, ranging from 1 to 10^7 copies per cell [18], mandates additional prefractionation methods [8] [12,16,38] or the utilisation of narrow pH strips [36] in order to display low-abundance to medium-abundance proteins. The enrichment of proteins by the PrepCell® system allowed, for instance, the detection of calcium-binding proteins such as calbindin and calretinin [7]. However, the PrepCell® allows only the separation according to protein mass. Another, more promising route will likely be the use of narrow range pH strips such as pH 4–7 and 6–9 and to subsequently zoom in further with strips of 1 pH unit. Finally, the analysis of narrowly defined functional areas, such as the MNTB or the LSO, will alleviate the detection of region-specific proteins.

In summary, our study presents the first proteome analysis of sensory brain areas. Our results demonstrate a great similarity between the expression pattern of major proteins in the SOC, the IC, and the cerebellum. Notable differences were observed as well, but these were mostly limited to proteins of medium and low abundance. Fifty protein spots were identified from the cytosolic fraction of the SOC. Further efforts are necessary to identify proteins which are differentially expressed between the SOC and IC, and between auditory and nonauditory centres. The results of this study will form the basis for the construction of a web-based integrated database of the gene repertoire of the auditory system in the brainstem (ID-GRAB, http://www/id-grab.de).

Acknowledgements

The monoclonal antibody a5 developed by Dr. Fambrough was obtained from the Developmental Studies Hybridoma Bank developed under the auspices of the NICHD and maintained by The University of Iowa, Department of Biological Sciences, Iowa City, IA 52242. We thank G. Schlenstedt for providing the anti-Hht1-C antibody.

References

[1] S. Beranova-Giorgianni, M.J. Pabst, T.M. Russell, F. Giorgianni, D. Goldowitz, D.M. Desiderio, Preliminary analysis of the mouse cerebellum proteome, Mol. Brain Res. 98 (2002) 135–140.
[2] L. Carboni, C. Piubelli, P.G. Righetti, B. Jansson, E. Domenici, Proteomic analysis of rat brain tissue: comparison of protocols for two-dimensional gel electrophoresis analysis based on different solubilizing agents, Electrophoresis 23 (2002) 4132–4141.
[3] J.H. Casseday, T. Fremouw, E. Covey, The inferior colliculus: a hub for the central auditory system, in: D. Oertel, R.R. Fay, A.A. Popper (Eds.), Springer Handbook of Auditory Research: Integrative Functions in the Mammalian Auditory Pathway, Springer, New York, 2002, pp. 238–318.
[4] G.D. Chermak, Deciphering auditory processing disorders in children, Otolaryngol Clin N Am 35 (2002) 733–749.
[5] G.L. Corthals, V.C. Wasinger, D.F. Hochstrasser, J.C. Sanchez, The dynamic range of protein expression: a challenge for proteomic research, Electrophoresis 21 (2000) 1104–1115.
[6] M. Fountoulakis, R. Hardmaier, E. Schuller, G. Lubec, Differences in protein level between neonatal and adult brain, Electrophoresis 21 (2000) 673–678.

[7] M. Fountoulakis, J.F. Juranville, Enrichment of low-abundance brain proteins by preparative electrophoresis, Anal. Biochem. 313 (2003) 267–282.
[8] M. Fountoulakis, J.F. Juranville, Enrichment of low-abundance brain proteins by preparative electrophoresis, Anal. Biochem. 313 (2003) 267–282.
[9] M. Fountoulakis, E. Schuller, R. Hardmeier, P. Berndt, G. Lubec, Rat brain proteins: two-dimensional protein database and variations in the expression level, Electrophoresis 20 (1999) 3572–3579.
[10] E. Friauf, Distribution of calcium-binding protein Calbindin-D_{28k} in the auditory system of adult and developing rats, J. Comp. Neurol. 349 (1994) 193–211.
[11] D.R. Frisina, R.D. Frisina, Speech recognition in noise and presbycusis—relations to possible neural mechanisms, Hearing Res. 106 (1997) 95–104.
[12] A. Görg, G. Boguth, A. Kopf, G. Reil, H. Parlar, W. Weiss, Sample prefractionation with Sephadex isoelectric focusing prior to narrow pH range two-dimensional gels, Proteomics 2 (2002) 1652–1657.
[13] B. Grothe, The evolution of temporal processing in the medial superior olive, an auditory brainstem structure, Prog. Neurobiol. 61 (2000) 581–610.
[14] J.W. Haycock, D.A. Haycock, Tyrosine hydroxylase in rat brain dopaminergic nerve terminals. Multiple-site phosphorylation in vivo and in synaptosomes, J. Biol. Chem. 266 (1991) 5650–5657.
[15] R.H. Helfert, C.R. Snead, R.A. Altschuler, The ascending auditory pathways, in: R.A. Altschuler (Ed.), Neurobiology of Hearing: The Central Auditory System, Raven Press, New York, 1991, pp. 1–25.
[16] B.R. Herbert, P.G. Righetti, A turning point in proteome analysis: sample prefractionation via multicompartment electrolyzers with isoelectric membranes, Electrophoresis 21 (2000) 3639–3648.
[17] D.R.F. Irvine, Physiology of the auditory brainstem, in: A.N. Popper, R.R. Fay (Eds.), The Mammalian Auditory Pathway: Neurophysiology, Springer, New York, 1992, pp. 153–231.
[18] J.R. Kettman, C. Coleclough, J.R. Frey, I. Lefkovits, Clonal proteomics: one gene-family of proteins, Proteomics 2 (2002) 624–631.
[19] G. Kim, K. Kandler, Elimination and strengthening of glycinergic/GABAergic connections during tonotopic map formation, Nature Neurosci. 6 (2003) 282–290.
[20] J. Klose, C. Nock, M. Herrmann, K. Stuhler, K. Marcus, M. Bluggel, E. Krause, L.C. Schalkwyk, S. Rastan, S.D.M. Brown, K. Bussow, H. Himmelbauer, H. Lehrach, Genetic analysis of the mouse brain proteome, Nature Genet. 30 (2002) 385–393.
[21] K. Krapfenbauer, M. Berger, G. Lubec, M. Fountoulakis, Changes in the brain protein levels following administration of kainic acid, Electrophoresis 22 (2001) 2086–2091.
[22] H. Langen, P. Berndt, D. Roder, N. Cairns, G. Lubec, M. Fountoulakis, Two-dimensional map of human brain proteins, Electrophoresis 20 (1999) 907–916.
[23] C. Lohmann, E. Friauf, Distribution of the calcium-binding proteins parvalbumin and calretinin in the auditory brainstem of adult and developing rats, J.Comp.Neurol. 367 (1996) 90–109.
[24] M. Mann, R.C. Hendrickson, A. Pandey, Analysis of proteins and proteomes by mass spectrometry, Annu. Rev. Biochem. 70 (2001) 437–473.
[25] G.L.G. Miklos, R. Maleszka, Protein functions and biological contexts, Proteomics 1 (2001) 169–178.
[26] J.E. Minturn, H.J. Fryer, D.H. Geschwind, S. Hockfield, TOAD-64, a gene expressed early in neuronal differentiation in the rat, is related to unc-33, a *C. elegans* gene involved in axon outgrowth, J. Neurosci. 15 (1995) 6757–6766.
[27] D. Oertel, R.R. Fay, A.N. Popper (Eds.), Integrative Functions in the Mammalian Auditory Pathway, Springer, New York, 2002.
[28] A. Reymond, V. Marigo, M.B. Yaylaoglu, A. Leoni, C. Ucla, N. Scamuffa, C. Cacciopoli, E.T. Dermitzakis, R. Lyle, S. Banfi, G. Eichele, S.E. Antonarakis, A. Ballabio, Human chromosome 21 gene expression atlas in the mouse, Nature 420 (2002) 582–586.
[29] A. Shevchenko, M. Wilm, O. Vorm, M. Mann, Mass spectrometric sequencing of proteins from silver stained polyacrylamide gels, Anal. Chem. 68 (1996) 850–858.
[30] I. Thalmann, H.L. Rosenthal, B.W. Moore, R. Thalmann, Organ of Corti-specific polypeptides: OCP-I and OCP-II, Arch Otorhinolaryngol. 226 (1980) 123–128.
[31] K. Tilleman, I. Stevens, K. Spittaels, H.C. Van den, S. Clerens, B.G. Van den, H. Geerts, F. Van Leuven, F. Vandesande, L. Moens, Differential expression of brain proteins in glycogen synthase kinase-3 β transgenic mice: A proteomics point of view, Proteomics 2 (2002) 94–104.
[32] K. Tilleman, H.C. Van den, H. Geerts, F. Van Leuven, E.L. Esmans, L. Moens, Proteomics analysis of the neurodegeneration in the brain of tau transgenic mice, Proteomics 2 (2002) 656–665.
[33] L.O. Trussell, Cellular mechanisms for preservation of timing in central auditory pathways, Curr. Opin. Neurobiol. 7 (1997) 487–492.
[34] L.O. Trussell, Synaptic mechanisms for coding timing in auditory neurons, Annu. Rev. Physiol. 61 (1999) 477–496.
[35] J.P. Walton, R.D. Frisina, W.E. Oneill, Age-related alteration in processing of temporal sound features in the auditory midbrain of the cba mouse, J. Neurosci. 18 (1998) 2764–2776.
[36] J.A. Westbrook, J.X. Yan, R. Wait, S.Y. Welson, M.J. Dunn, Zooming-in on the proteome: very narrow-range immobilised pH gradients reveal more protein species and isoforms, Electrophoresis 22 (2001) 2865–2871.
[37] T.C.T. Yin, Neural mechanisms of encoding binaural localization cues in the auditory brainstem, in: D. Oertel, R.R. Fay, A.A. Popper (Eds.), Springer Handbook of Auditory Research: Integrative Functions in the Mammalian Auditory Pathway, Springer, New York, 2002, pp. 99–159.
[38] X. Zuo, L. Echan, P. Hembach, H.Y. Tang, K.D. Speicher, D. Santoli, D.W. Speicher, Towards global analysis of mammalian proteomes using sample prefractionation prior to narrow pH range two-dimensional gels and using one-dimensional gels for insoluble and large proteins, Electrophoresis 22 (2001) 1603–1615.